Vet. Pathol. 26:303–308 (1989)

Magnetic Resonance Imaging of Hepatic Neoplasms in the Rat

G. A. JOHNSON, M. B. THOMPSON, G. P. COFER, D. CAMPEN, AND R. R. MARONPOT

Department of Radiology, Duke University Medical Center, Durham, NC; and National Institute of Environmental Health Sciences, Research Triangle Park, NC

Abstract. Magnetic resonance imaging (MRI) at microscopic resolution was done on a live rat that had chemically induced hepatic neoplasms. Beginning at the anterior aspect of the liver, 16 contiguous transaxial slices (each 1.25 mm thick) were produced using three-dimensional Fourier transform sequences. The rat had been treated with diethylnitrosamine (200 mg/kg) at 70 days of age, and, subsequently, received periodic implants of 17a-ethynylestradiol for 60 weeks. Carr-Purcell-Meiboom-Gill (CPMG) sequences (repetition time = 2,000 and echo time = 20, 40, 60, 80 ms) were done to give quantitative measures of spin-spin relaxation times (T2). Pixel-by-pixel curve fitting from these multiple images yielded calculated T2 images. Histologic evaluation of three abnormal areas in the liver revealed solid and cystic hepatocellular adenomas. Although lesions were evident in early-echo images of the CPMG sequence, they were more apparent in the late-echo images. This was consistent with longer T2 relaxation times for the lesions. The voxels of dimensions (230 × 230 × 1,250 μm) permitted resolution of volume elements <0.07 mm^3. This in turn permitted clear delineation of focal lesions <3 mm in diameter. The potential for MRI at microscopic resolution in toxicologic research is clearly demonstrated.

Since its inception in 1973,[15] magnetic resonance imaging (MRI) has developed rapidly as a clinical tool.[14,17] A subject is placed in a strong magnetic field which causes the hydrogen protons to precess synchronously about the direction of the applied field. A pulse of radiowaves at the same frequency as this synchronous precession is applied to stimulate the protons. A short time later, a radiofrequency echo is generated in the tissue. This signal is spatially encoded by a suitable series of magnetic field gradients. Detection and analysis of this signal permits the construction of a two-dimensional image of the selected plane through the subject. Thorough discussions of the technology have been presented.[14,17]

Recently, because of improvements in resolution, the use of MRI in nonclinical areas has been explored.[1,5,8,11–13] Our goal has been to develop MRI at microscopic resolution as a noninvasive technique for use in toxicologic research with rats. Important applications would include the abilities to detect chemically induced neoplasms, to characterize these lesions, and to follow the development of a neoplasm, with or without modification of treatment, over time in the same animal. Here we report the detection of small to moderately sized chemically induced lesions (3–20 mm in diameter), and demonstrate the potential for characterizing these lesions using the spin-spin relaxation time (T2).

Materials and Methods

Treatment

Ovariectomized Sprague-Dawley rats were acquired from Charles River Breeding Laboratory, Kingston, New York. The rat used in this study was housed in a controlled environment with three others (four per cage) that received similar treatment. The rats had free access to food (NIH-31, Zeigler Brothers, Gardner, PA) and water. At 70 days of age, the rats were injected intraperitoneally with 200 mg/kg of diethylnitrosamine (Sigma Chemical Co., St. Louis, MO). At 80 days of age, and every 28 days thereafter, Silastic capsules containing 8 mg of a ground, homogenized mixture of 17a-ethynylestradiol (EE2) were implanted subcutaneously at the back of the neck. Medical grade Silastic tubing and adhesive for preparation of capsules were obtained from Dow Corning Corporation, Midland, Michigan. Cholesterol and EE2 were obtained from Steraloids, Inc., Wilton, New Hampshire. Complete and consistent release of EE2 from the capsule over a 28-day period would have resulted in a dose of 37 μg EE2/kg/day. The rat imaged in this experiment was treated for 60 weeks. Five days after imaging, the rat was killed, and sections of liver that contained gross abnormalities were fixed in 10% buffered formalin and processed for routine staining with hematoxylin and eosin.

Nuclear magnetic resonance imaging

All imaging was done on a 2.0 Tesla chemical shift imaging device (General Electric NMR Instruments, Freemont, CA) being developed for magnetic response (MR) microscopy. To

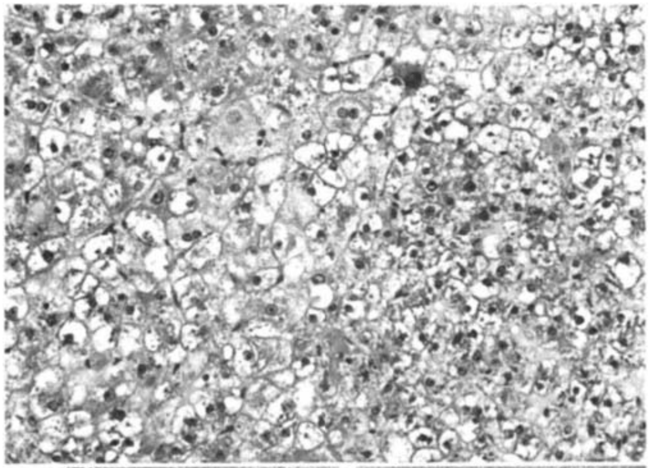

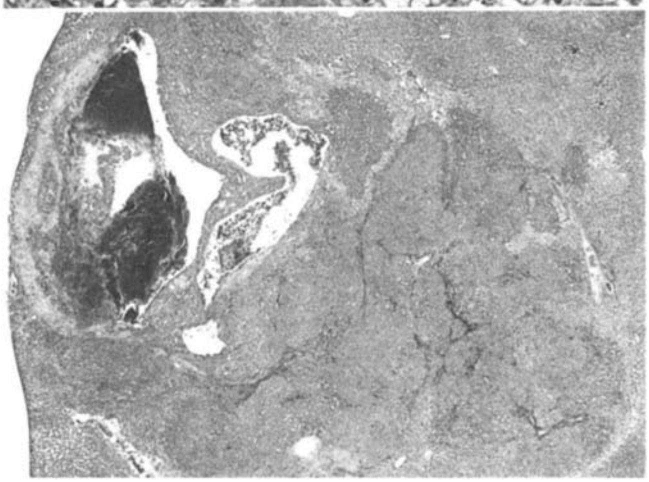

Fig. 1. Liver. Hepatocellular adenoma designated "A" (Fig. 4), right anterior lobe. Neoplasm is comprised of vacuolated hepatocytes arranged uniformly without an apparent lobular pattern. HE.

Fig. 2. Liver. Hepatocellular adenoma designated "B" (Fig. 4), medial lobe. Neoplasm has an irregular lobular pattern and contains blood-filled cysts. HE.

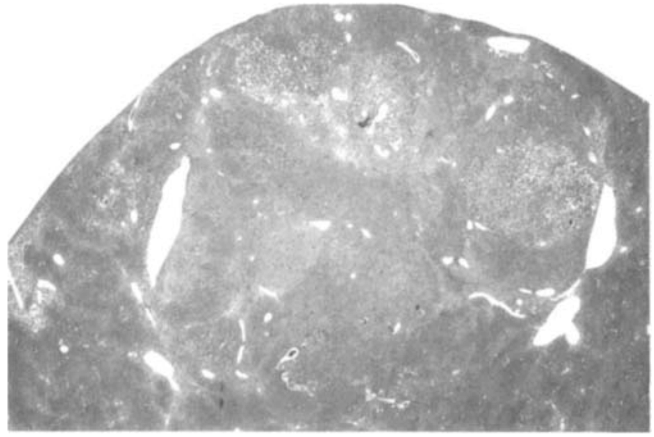

Fig. 3. Liver. Hepatocellular adenoma designated "C" (Fig. 4), left lobe. This poorly circumscribed neoplasm contains regions of sinusoidal dilatation. HE.

improve signal detection, special radiofrequency (rf) coils have been constructed to efficiently capture the weak signal from the animal being studied. The cylindrical coils, 6.0 cm in diameter by 8.0 cm in length, are scaled versions of the "birdcage" design developed by Hayes et al., for clinical imaging of the whole body.[6]

Spatial encoding was accomplished using a three-dimensional imaging technique (3DFT) which, in this study, allowed the simultaneous imaging of 16 contiguous planes (each 1.25 mm thick) through the rat.[4,10,12] Each slice had a 60-mm field of view and was reconstructed on a 256 × 256 matrix. This produced pixels with dimensions of 234 × 234 × 1,250 μm (0.07 mm^3).

The 3DFT is susceptible to motion artifacts produced by breathing and vascular pulsation. This problem was minimized by controlling the respiratory cycle of the rat with the MR system. The animal was intubated through the trachea with a #5 quick catheter, approximately 4 cm in length. The catheter was connected to a pulsed ventilation system that supplied an oxygen-halothane mixture for anesthesia. This apparatus was triggered by the MR system which was pulsing at a rate of 0.5–4.0 cycles/second. An MR pulse sequence began with rf excitation, a delay of 20–100 ms, and capture of the rf echoes. The protons recovered for an additional 1.9 seconds, during which time the respirator was pulsed. This triggered the forced ventilation cycle after which the next segment of the MR pulse sequence began. By control of the respiratory pulse duration and timing, motion was minimized during the crucial 100 ms when MR excitations and signal detection occurred. This technique has been previously described.[7,8] This study, which required 8,192 pulses for the volumetric image set, required a total scan time of approximately 5 hours.

The intensity of a point in an image depends upon several variables of the tissue, notably the relative proton concentration, the spin lattice relaxation time (T1), and spin-spin relaxation time (T2). The relative significance of these factors is determined by the timing in the pulse sequence (repetition time [TR] and echo time [TE]) in which TE is the time between initial rf excitation and reception of the spin echo signal, and TR is the time between each of the multiple rf excitations required for spatial encoding. Investigators have discovered that many hepatic lesions have prolonged T1 and T2.[3,9,18,19] One of the exciting potentials for such studies is the ability to alter the image contrast through selection of the timing parameters of the sequence. Accordingly, either a T1 weighted sequence (short TR, short TE) or a T2 weighted sequence (long TR, long TE) could be appropriate. We used a Carr-Purcell-Meiboom-Gill (CPMG) sequence which generated four images (TE = 20, 40, 60, 80 ms) at each level (slice) in the rat. This sequence dramatically demonstrates the effects that different timing (TE) has on the image contrast (Figs. 4a, b; 5a, b).

Increasing the length of echo time produces images that are progressively dependent on differences in tissue T2. By fitting the signal intensity in each pixel to a function ($e^{-TE/T2}$), a calculated T2 image can be produced in which the intensity of any point in the image is the T2 of the tissue at that point.[16] In the current study, TR of 2,000 ms was used, which allowed most protons to return to equilibrium (relaxation) before the next pulse sequence was initiated. Consequently, T1 dependence was minimal.

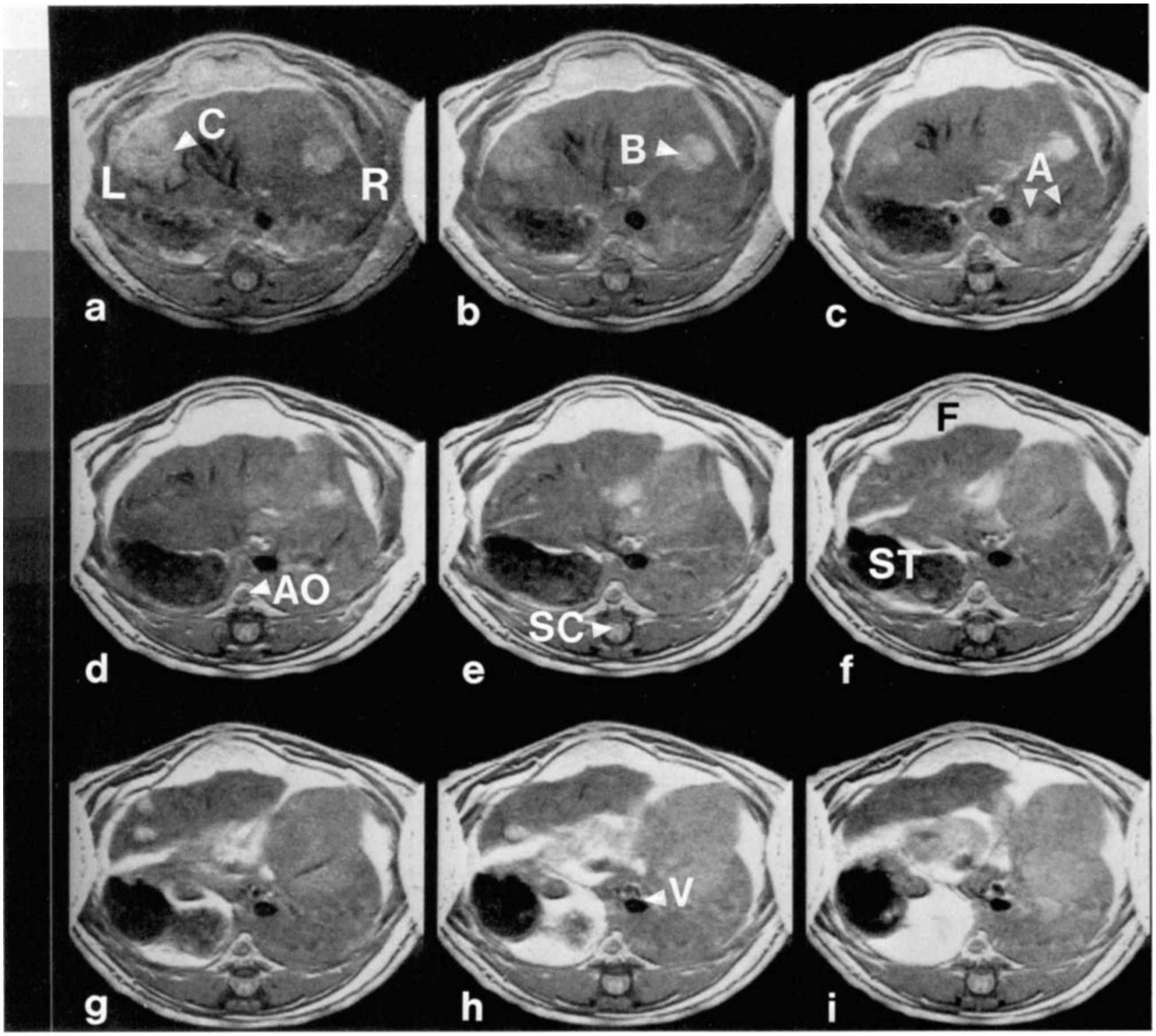

Fig. 4. Nine contiguous 1.25-mm-thick images (a–i) from first echo (TE = 20 ms) of three-dimensional Carr-Purcell-Meiboom-Gill sequence. Clearest images of each neoplasm are identified by (A), (B), and (C). Anatomic structures are aorta (AO), stomach (ST), vein (V), spinal cord (SC), and fat (F).

Results

Gross and histopathologic findings

The right anterior lobe of the liver contained a 2-cm diameter solid mass (labeled as "A" in the magnetic resonance image, Fig. 4) consisting of vacuolated, glycogen-filled hepatocytes arranged uniformly without an apparent lobular pattern (Fig. 1). This hepatocellular adenoma was clearly demarcated with moderate compression of surrounding non-vacuolated hepatic parenchymal cells. The central portion of the median lobe had an 8-mm diameter mass composed of basophilic hepatocytes arranged in an irregularly lobular pattern. This lesion, designated adenoma "B" in Fig. 4, compressed the surrounding parenchyma and contained a blood-filled cavity approximately 2 mm in diameter (Fig. 2). The apex of the left lobe contained a grossly pale mass approximately 1.5 cm in diameter. This mass, designated hepatocellular adenoma "C" in Fig. 4, was poorly circumscribed and contained focal regions of sinusoidal dilatation that were 2–4 mm in diameter separated by compact zones of basophilic hepatocytes (Fig. 3).

Magnetic resonance (MR) terminology

The goal of this work is to demonstrate to the pathology community the potential for MR in detecting and characterizing lesions. We provide a brief glossary to remove the barrier imposed by the MR terminology:

Spatial encoding. The process of generating an im-

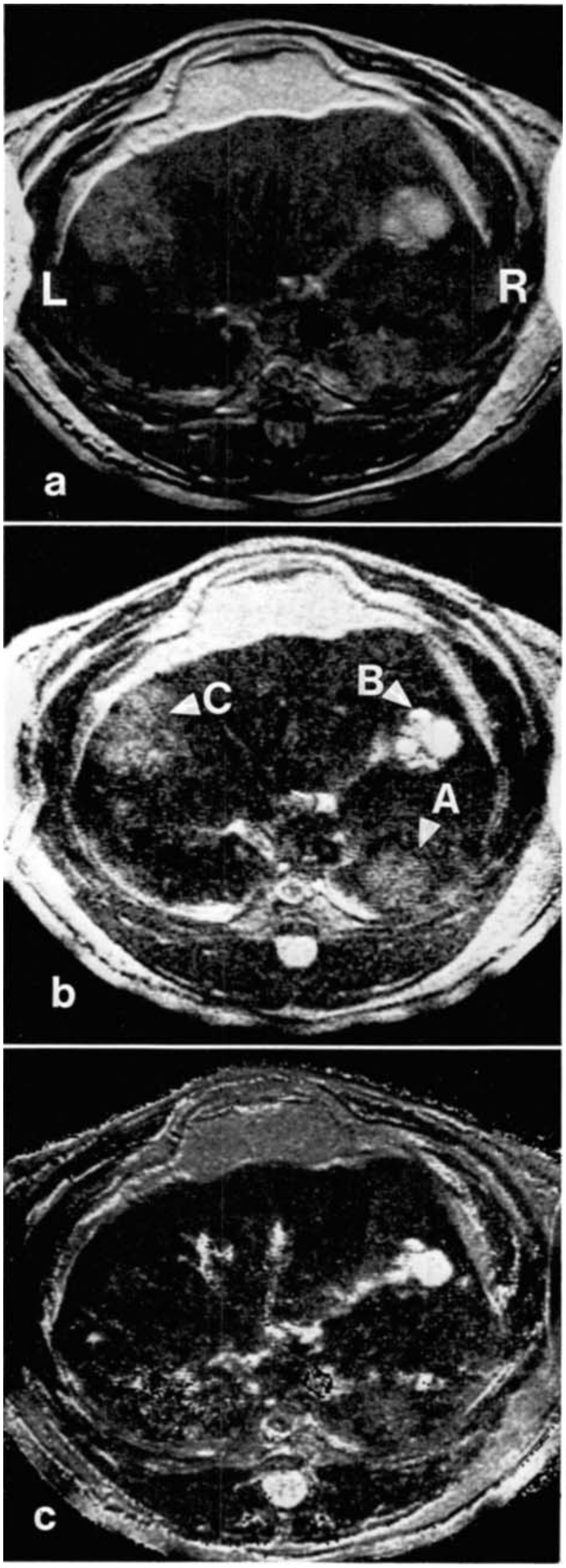

Fig. 5. Short and long echo and calculated T2 images of the level in Fig. 4b. Neoplasms (A), (B), and (C) are identified. (a) The first echo (echo time [TE] = 20 ms) of Carr-Purcell-Meiboom-Gill (CPMG) set. (b) The third echo (TE = 60 ms) of CPMG set. Here the differential relaxation between normal liver and lesions permits better definition of the neoplasms. (c) Pixel-by-pixel calculated T2 image. Adenoma "B," which is cystic, is well defined.

age. It is accomplished through a sequence of magnetic gradient and radiofrequency (rf) pulses that delineate the signal from individual points of the sample.

Slice. MR is a tomographic technique, i.e., a technique which allows selection of a single plane for imaging and the removal of overlying and underlying structures. Just as histology specimens have some finite thickness, so too do these images. In this work, the effective slice thickness is 1,250 μm. This slice definition is done by the magnetic gradient and can, therefore, be done without killing the animal.

Pixels. The individual points of the digital image. While the image appears to be a continuum, it is in fact a *matrix,* i.e., an array of discrete points. Typically, this array consists of 256 rows with 256 columns. The signal intensity for a discrete volume of the tissue is assigned to each of these picture elements. The stronger signals are represented by brighter pixels.

Voxel. The volume of tissue that is represented by each pixel. In this work each pixel represents the signal from a cube of tissue 234 × 234 × 1,250 μm.

T1, T2, N(H), repetition time (TR), echo time (TE). The signal intensity of any pixel depends in a complex fashion on the intrinsic properties of the tissue (T1, T2, and N[H]), and on the timing of the sequence used in the spatial encoding (TE and TR). The tissue is initially excited by an rf pulse. Shortly thereafter a second rf pulse stimulates the tissue to yield a returned rf signal, i.e., an *echo.* The time between initial excitation and the echo is *TE.* In the pulse sequence used here, additional rf pulses were applied to stimulate echos at later periods (longer TE). An additional period in the sequence, *TR,* follows, during which the protons recover from the initial excitation. The protons in different tissues decay and recover at different rates. The fact that these rates differ substantially among tissues accounts for the contrast between tissues seen in the images and leads to the potential for characterizing these tissues. *T1,* the spin lattice relaxation is related to the degree to which water is bound in the tissue.[9,14,17] The degree to which an image depends on T1 is determined by TR—short TR yields an image dependent on T1; long TR removes this dependence. *T2,* the spin-spin relaxation time, is a measure of how quickly the signal decays after excitation. It is generally shorter for tissues that are more solid. T1 and T2 can both be affected by the presence of paramagnetic species, the most prominent of which is Fe. As iron changes its oxidation state (from Fe^{2+} to Fe^{3+}), it decreases both

T1 and T2 in the surrounding tissue.[2] Finally, the signal from any point is directly related to the *N(H)*, the relative proton density, i.e., the number of protons in that voxel.

MR images

Nine contiguous images from the first echo (TE = 20 ms, TR = 2,000 ms) in the Carr-Purcell-Meiboom-Gill sequence were selected (Fig. 4). These images span a longitudinal distance of 1.125 cm in the anterior abdomen of the rat and demonstrate the volumetric coverage of the technique. Anatomic landmarks include stomach, spinal cord, aorta, and hepatic veins. The most intense (bright) normal tissue is fat, which has high relative proton density, a T1 shorter than most of the surrounding tissues, and a T2 longer than that of most of the surrounding tissues. The three areas that were noted grossly and described histologically (A, B, and C in Figs. 1–3) were detected as areas of increased signal intensity in this series of images. Additionally, focal lesions ranging from approximately 3 to 5 mm in diameter were detected (Fig. 4f, g).

Tissues and lesions with long T2 become increasingly differentiated from other tissues as the TE is increased. At level b in Fig. 4, comparisons were made of details and characteristics of images for (a) a short echo (TE = 20 ms, TR = 2,000 ms) and (b) a longer echo (TE = 60 ms). These images are shown in Fig. 5. Figures 4b and 5a are the same images. The display parameters are altered slightly in Fig. 5a to permit comparison with Fig. 5b. Compared to 5a, the image in 5b is grainier (poor signal to noise) because the signal from all the tissues has decayed exponentially (longer TE). However, because signal from normal hepatic tissue (T2 ~ 40 ms) decays more quickly than that in tissues (including lesions) with longer T2 (~60–80 ms), the contrast between lesions and normal parenchyma is actually greater.

Figure 6 shows a similar comparison of (a) short echo (TE = 20 ms) and (b) long echo (TE = 60 ms) at another level with three other small lesions (arrows) believed to represent small hepatocellular adenomas. As in Fig. 5, the lesions with longer T2 show up more clearly in the image with the longer echo (Fig. 6b). Figure 6c shows the pixel-by-pixel calculated T2 image. The calculated T2 image shows that all of the lesions have T2 longer than that of any other tissue in the image.

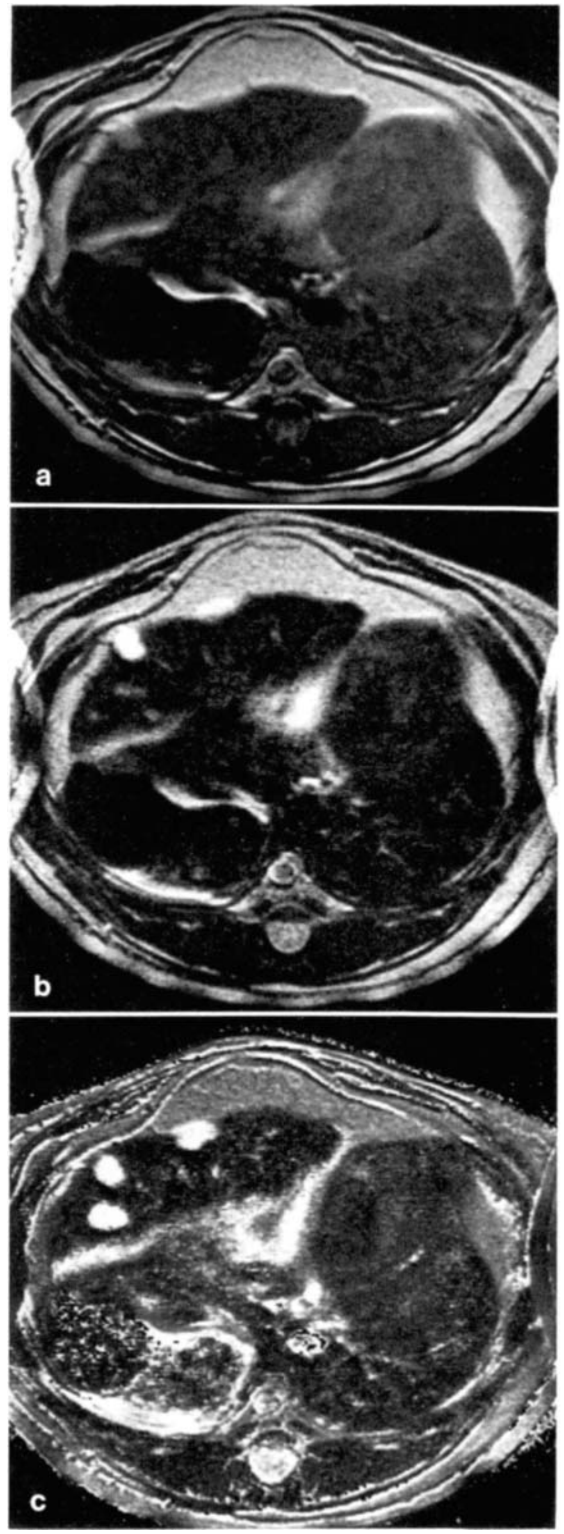

→

Fig. 6. Comparison of short and long echo and calculated T2 images at level f in Fig. 4. Although histologic confirmation of the diagnosis for these specific small lesions was precluded by the tissue being used for biochemical assays, similarly sized lesions produced by the experimental protocol previously have been shown to be large foci of cellular alteration or early small hepatocellular adenomas. (a) The first echo (echo time [TE] = 20 ms) of the Carr-Purcell-Meiboom-Gill (CPMG) set. (b) The third echo (TE = 60 ms) of the CPMG set. Note better definition of the lesions as a consequence of their longer T2. (c) Pixel-by-pixel calculated T2. All lesions have T2 longer than any other tissue (including fat) in the image.

Discussion

All of the lesions were seen as a consequence of prolonged T2 relative to surrounding normal parenchyma. Indeed, in Fig. 6, the T2 of these lesions is longer than any of the other tissues. A number of investigators have suggested that T1 and T2 might be very specific tissue markers.[3,9,18,19] While it is clear that magnetic resonance (MR) is a sensitive technique, it is not clear that it is specific. Earlier efforts showed some degree of correlation between pathology and T1 and T2, but the degree of specificity necessary for accurate histological identification has not been achieved. The images shown here are acquired with voxels that are 60 to 100 times smaller than earlier efforts.[3,9] It may be possible to translate this increased resolution to a greater degree of specificity. Efforts are under way now to do so.

This work has demonstrated the ability to noninvasively detect chemically induced hepatic lesions as small as 3 mm in diameter in the live rat. By using thin slices (1.25 mm), volume averaging of lesions was reduced and contrast was improved greatly. Excellent signal-to-noise ratio was achieved through the use of three-dimensional imaging. Multiple images were acquired at several points in the T2 relaxation curve by use of the Carr-Purcell-Meiboom-Gill radio frequency pulse sequence. Use of gated ventilation allowed the animals to be anesthetized and imaged for extended periods (4 to 5 hours) and recovered for continued investigations. In toxicology experiments, this will permit the longitudinal characterization of abnormalities (progression, regression) produced by continuation or modification of a treatment. Continued refinement of the technique will provide a new dimension in toxicological research.

Acknowledgements

The authors thank Dr. Larry Hedlund, Ms. Gilda Mills, and Ms. Deborah Moore for animal anesthesia and care. This work was supported in part by NIEHS contract #273-87-P-0024 and NIH grant RO1-ES04187.

References

1 Aguayo JB, Blackband SJ, Schoeniger J, Mattingly MA, Hintermann M: Nuclear magnetic resonance imaging of a single cell. Nature **322**:190–191, 1986

2 Brooks R, DiChiro G: Magnetic resonance imaging of stationary blood: a review. Med Phys **14**(6):903–913, 1987

3 Davis P, Kaufman L, Crooks LE, Miller TR: Detectability of hepatomas in rat livers by nuclear magnetic resonance imaging. Invest Radiol **16**:354–358, 1981

4 den Boef JH, van Uijen CMJ, Holzscherer CD: Multiple slice NMR imaging by three-dimensional Fourier zeumatography. Phys Med Biol **29**:857–867, 1984

5 Eccles CD, Callaghan PT: High resolution imaging: the NMR microscope. J Magn Res **68**:393–398, 1986

6 Hayes CE, Edelstein WA, Schenk JF, Mueller OM, Eash M: An efficient highly homogeneous radiofrequency coil for whole body NMR imaging at 1.5 T. J Magn Res **63**: 622–628, 1985

7 Hedlund L, Dietz J, Nassar R: A ventilator for magnetic resonance imaging. Invest Radiol **21**:18–23, 1986

8 Hedlund LW, Johnson GA, Mills GI: Magnetic resonance microscopy of the rat thorax and abdomen. Invest Radiol **21**:843–846, 1986

9 Herfkens RJ, Davis PL, Crooks LE: NMR imaging of the abnormal live rat and correlation with tissue characteristics. Radiology **141**:211–218, 1981

10 Johnson G, Hutchison JMS, Redpath TW, Eastwood LM: Improvements in performance time for simultaneous three dimensional NMR imaging. J Magn Res **54**: 374–384, 1983

11 Johnson GA, Brown J, Kramer PJ: Magnetic resonance microscopy of changes in water content in stems of transpiring plants. Proc Natl Acad Sci (USA) **84**:2752–2755, 1987

12 Johnson GA, Thompson MB, Drayer BP: Three dimensional MRI microscopy of the normal rat brain. Magn Reson Med **4**:351–365, 1987

13 Johnson GA, Thompson MB, Gewalt SL, Hayes CE: Nuclear magnetic resonance at microscopic resolution. J Magn Res **68**:129–137, 1986

14 Kressel HY: Magnetic Resonance Annual. Raven Press, New York, 1986

15 Lauterbur PC: Image formation by induced local interactions: examples employing nuclear magnetic resonance. Nature **242**:190–191, 1973

16 MacFall J: Pulse sequence considerations for computed T1, T2, and spin density images. *In:* The Technology of Nuclear Magnetic Resonance, ed. Esser PD and Johnston RE, pp. 79–96. Society of Nuclear Medicine, New York, 1984

17 Mansfield P, Morris PG: NMR Imaging in Biomedicine. Academic Press, New York, 1982

18 Ohtomo K, Itai Y, Furiu S, Yashiro N, Yoshikawa K, Lio M: Hepatic tumors: differentiation by transverse relaxation time (T2) of magnetic resonance imaging. Radiology **155**:421–423, 1985

19 Stark DD, Bass NM, Moss AA: Nuclear magnetic resonance imaging of experimentally induced liver disease. Radiology **148**:743–751, 1983

Request reprints from Dr. G. A. Johnson, Department of Radiology, PO Box 3302, Duke University Medical Center, Durham, NC 27710 (USA).